Deamination of Protonated Amines to Yield Protonated Imines

Duxi Zhang, L. A. Gill, and R. G. Cooks
Department of Chemistry, Purdue University, West Lafayette, Indiana, USA

Primary and secondary amines, when examined in atmospheric pressure chemical ionization, electrospray ionization, or chemical ionization, display protonated imines in their mass spectra. These products arise formally by nucleophilic substitution at the α-carbon with loss of both ammonia and molecular hydrogen. Collision-induced dissociation (CID) is used to characterize the product ions by comparison with authentic protonated imines. Gas-phase ion/molecule reactions of protonated amines with neutral amines also yield products that correspond to protonated imines (deamination and dehydrogenation), as well as providing simple deamination products. The reaction mechanism was investigated further by reacting the deamination product, the alkyl cation, with a neutral amine. The observed dehydrogenation of the nascent protonated secondary amine indicates that the reaction sequence is loss of ammonia followed by dehydrogenation even though the isolated protonated secondary amines did not undergo dehydrogenation upon CID. Formation of the deamination products in the protonated amine/amine reaction is competitive with proton-bound dimer formation. The proton-bound dimers do not yield deamination products under CID conditions in the ion trap or in experiments performed using a pentaquadrupole instrument. This demonstrates that the geometry of the proton-bound dimer, in which the α-carbons of the alkylamines are well separated [C_α—N—H—N—C_α], is an unsuitable entry point on the potential energy hypersurface for formation of the imine [C_α—N—C_α]. Isolation of the proton-bound dimers in the quadrupole ion trap is achieved with low efficiency and this characteristic can be used to distinguish them from their covalently bound isomers. (J Am Soc Mass Spectrom 1998, 9, 1146–1157) © 1998 American Society for Mass Spectrometry

Ion/molecule reactions have been widely used in analytical and organic mass spectrometry, especially since the introduction of the chemical ionization (CI) technique by Munson and Field in 1966 [1]. In spite of this, the ion/molecule chemistry of simple amines has not been studied extensively [2] and surprising results, like the new reaction reported here, can still be encountered. Compared to extensive studies of the behavior of protonated aliphatic alcohols [3, 4], which undergo characteristic dehydration, there is limited information on the chemical ionization of aliphatic amines. Deamination is not usually a major process in the CI spectra of amines [5, 6], although Reiner et al. [6] showed that under H_2 CI conditions the $(MH–NH_3)^+$ ion has a relative abundance of 23% for *n*-butylamine and is the base peak for *n*-propylamine. Appropriate α-substituents can stabilize the products and increase the tendency for ammonia loss in amine CI spectra [7]. The bimolecular chemistry of protonated amines with neutral amines also contrasts with the corresponding alcohols. Protonated alcohols react with their neutral counterparts by nucleophilic substitution with accompanying dehydration [8]. The corresponding deamination reaction in the amine case is not nearly as facile. Depending on the amine partial pressure, ion/molecule reactions including those performed in the CI source yield proton-bound dimers of alkylamines in high yield. These ions have been studied extensively in the course of measurements of proton affinities by the kinetic method [9–12] using various types of ion sources and mass spectrometers. Characteristically, these ions dissociate to yield only the protonated monomers as dissociation products; in particular they do not yield deamination products. This result is also in contrast to those for the proton-bound dimers of the alcohols, which yield dehydration products [8]. There appear to be no previous reports on ammonia elimination in the course of ion/molecule reactions between protonated alkylamines and the corresponding neutral molecules. Although intermolecular deamination is not characteristic of alkylamine CI mass spectra, intramolecular loss of ammonia is a major process in some polyfunctional compounds, including diamines [13], α,ω-hydroxylamines [14], α,ω-amino alcohols and α,ω-amino acids [15], and α-amino acids and their derivatives [16].

In the current study, an ion trap mass spectrometer [17–19] was employed with atmospheric pressure chemical ionization (APCI) and electrospray ionization (ESI), initially in an attempt to generate proton-bound

Address reprint requests to R. G. Cooks, Department of Chemistry, Purdue University, West Lafayette, IN 47907-1393. E-mail: cooks@purdue.edu

© 1998 American Society for Mass Spectrometry. Published by Elsevier Science Inc.
1044-0305/98/$19.00
PII S1044-0305(98)00093-2

Received August 28, 1997
Revised June 29, 1998
Accepted July 6, 1998

dimers and study amine ion/molecule chemistry. Under certain conditions, abundant ions, which are formally the products of ammonia and subsequent hydrogen losses from proton-bound dimers of amines, were observed in the mass spectra. Therefore, the study was redirected toward identification of these ions, elucidation of the conditions favoring their formation and investigation of some aspects of the reaction mechanism. The reactions under investigation appear to be nucleophilic substitutions of the type:

$$R_1\text{–}CH_2\text{–}NH_3^+ + R_2\text{–}CH_2\text{–}NH_2 \rightarrow R_1\text{–}CH_2\text{–}NH_2^+\text{–}CH_2\text{–}R_2 + NH_3 \quad (1)$$

where the product ion apparently undergoes further fragmentation:

$$R_1\text{–}CH_2\text{–}NH_2^+\text{–}CH_2\text{–}R_2 \rightarrow \begin{cases} R_1\text{–}CH_2\text{–}NH^+\text{=}CH\text{–}R_2 + H_2 \\ R_1\text{–}CH\text{=}NH^+\text{–}CH_2\text{–}R_2 + H_2 \end{cases} \quad (2)$$

Mechanistic experiments were performed using CI in a triple quadrupole and a pentaquadrupole instrument and these revealed some unexpected features of the reactions.

Experimental

APCI and ESI experiments were carried out using an LCQ system (Finnigan, San Jose, CA) equipped with either an APCI source or an ESI source. Operating conditions for the APCI source were as follows: source voltage, 5 kV; source current, 5 μA; vaporizer temperature, 450°C; sheath and auxiliary gas (N_2) flow rates, 70 and 5, respectively (manufacturer's arbitrary units); capillary voltage, 4 V; capillary temperature, 150°C; maximum ion injection time, 400 ms; automatic gain control, 1×10^8 counts for a full-scan mass spectrum and 5×10^7 counts for a full-scan MS/MS experiment. The ESI conditions were as follows: spray voltage, 3.5 kV; sheath and auxiliary gas (N_2) flow rates, 80 and 20, respectively (manufacturer's arbitrary units); capillary voltage, 3 V; capillary temperature, 200°C; maximum ion injection time, 400 ms; automatic gain control, 5×10^7 counts for a full-scan mass spectrum. An MP-80 HPLC pump (BAS, West Lafayette, IN) was used to deliver the mobile phase to the LCQ. For the APCI experiments, the mobile phase was a 50:50 methanol/water solution with 1% acetic acid and the flow rate was 1.0 mL/min. For the ESI experiments the mobile phase was a 50:50 methanol/water and the flow rate was 0.4 mL/min. In both experiments the samples were manually loaded into the system through a 5 μL injection loop.

For the analytical scans performed using the LCQ, the q_z values for isolation, resonance excitation, and ejection are 0.8, 0.25, and 0.9, respectively. The excitation time for collision-induced dissociation (CID) was 30 ms. Data were acquired using the LCQ software in the full-scan mass spectrum or MS/MS mode and spectra were generated after appropriate background subtraction. The spectra reported represent averaged data taken over the period of sample introduction. In the full-scan MS/MS mode, the parent ion of interest was first isolated by applying an appropriate waveform across the endcap electrodes of the ion trap to resonantly eject all trapped ions except those of interest. The isolated ions were then subjected to a supplementary ac signal to resonantly excite them and cause collision-induced dissociation (CID). The amplitude of the ac used for CID was optimized in each experiment and both this value and the manufacturer's nominal relative collision energy (%) are reported. (The range from 0 to 100% relative collision energy corresponds to 0 to 5 V peak-to-peak resonant excitation potential.)

The triple quadrupole instrument used was a TSQ700 (Finnigan, San Jose, CA) operated under self-CI conditions. In these experiments the source temperature was 100°C, the manifold temperature was 70°C and, for the MS/MS experiments, a nominal 0.4 mtorr of argon was used as the collision gas. Reagents were introduced directly into the ion source through a Granville Philips leak valve. Mechanistic studies were carried out using a home-made pentaquadrupole instrument [20] and a Finnigan MAT (San Jose, CA) ITS 40 ion trap mass spectrometer with internal ionization. Self-CI was employed in the pentaquadrupole instrument and in the ITS ion trap. In the ITS ion trap, the q_z values for isolation, resonance excitation, and ejection of ions in the analytical scans were 0.78, 0.3, and 0.89, respectively.

All compounds were commercially available except for the imines, which were prepared by simply mixing equal amounts of the appropriate amine and aldehyde or ketone. The resulting reactions are exothermic and after cooling the reaction mixture, the water-insoluble products were isolated by removing the water produced by the reaction using a syringe. A small amount of anhydrous sodium sulfate was then added to absorb the residual water. The imines were not purified but simply diluted to 2% by volume with methanol. The amine samples were also diluted to 2% by methanol for use in the APCI and ESI experiments. In some experiments lower concentrations were used but much lower abundance protonated imines were formed. Data are shown in thomson, where 1 thomson (Th) = 1 Da per charge [21].

Results and Discussion

Formation of (2M+1–19)$^+$ Ions

Straight-chain alkylamines were found to yield protonated amines, when examined by APCI using an acidic mobile phase. Even under conditions where they yielded only low abundance proton-bound dimers, abundant ions with masses 19 Da less than the corresponding proton-bound dimers, i.e., (2M+1–19)$^+$ ions where the M denotes the molecular weight of the amine, were observed. In the representative case of *n*-butylamine, the (2M+1–19)$^+$ ion (128 Th), was one of the most abundant ions in the mass spectrum, whereas the abundance of the proton-bound dimer, (2M+1)$^+$ (147 Th), was only 4% to 5% of the *m/z* 128 ion abundance. Other amines such as *n*-propylamine, *n*-amylamine, and *n*-hexylamine also showed abundant (2M+1–19)$^+$ ions with limited signals for the proton-bound dimers. The formation of heterodimers (mixed proton-bound cluster ions) and the mixed deamination products was investigated using mixtures of amines. For mixtures of any two amines, the resulting spectrum showed three (2M+1–19)$^+$ ions that corresponded to the loss of 19 Da from the three possible proton-bound dimers, i.e., from the two homodimers and the heterodimer. To determine if the reaction is limited to straight-chain alkyl amines, a mixture of two cycloamines, cycloheptylamine and cyclooctylamine, was examined. The same pattern of (2M+1–19)$^+$ ion abundance was again obtained with this mixture.

Typical APCI mass spectra for representative mixtures of alkylamines and cycloalkylamines are reproduced in Figure 1. The mixture of *n*-propylamine and *n*-butylamine (Figure 1a) shows the protonated monomers (60 and 74 Th) and abundant ions at 100, 114, and 128 Th, corresponding to the loss of ammonia and molecular hydrogen from the proton-bound dimer of *n*-propylamine, the heterodimer of *n*-butylamine and *n*-propylamine, and the homodimer of *n*-butylamine, respectively. On the other hand, the corresponding proton-bound dimers themselves occur in abundances less than 4% of the base peak. The APCI mass spectrum of a mixture of two cyclic amines, shown in Figure 1b, exhibits (2M+1–19)$^+$ ion formation to an even more pronounced degree: the three (2M+1–19)$^+$ ions, 208, 222, and 236 Th, dominate the spectrum with the base peak being the ion at *m/z* 222. Only one proton-bound dimer (255 Th) is observed and it has less than 1% of the base peak abundance. The pattern of very weak proton-bound dimers and very abundant (2M+1–19)$^+$ ions was a feature of the spectra of all the pure amines and amine mixtures examined under the chosen conditions. The results for a number of amines and amine mixtures are summarized in Table 1. Data taken using ESI and CI are presented in a later section.

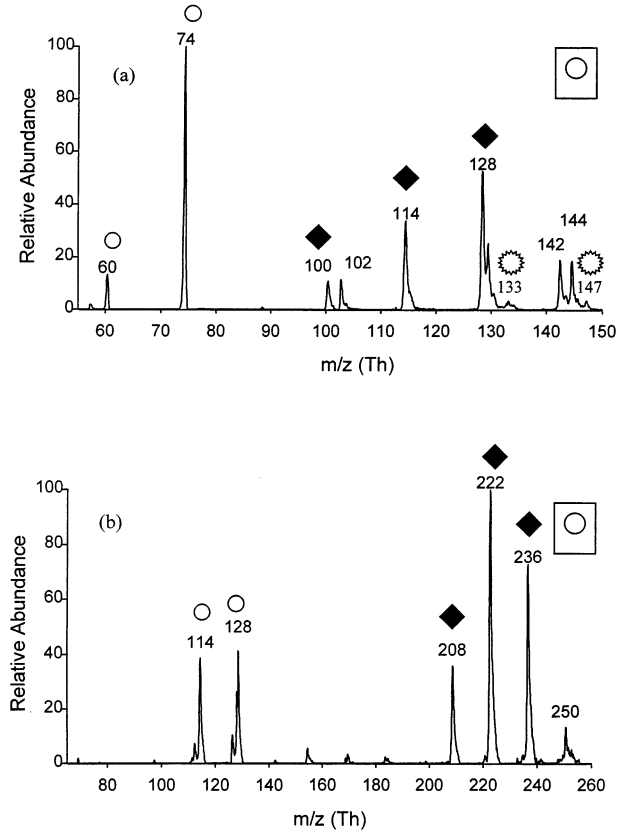

Figure 1. Formation of (2M+1–19)$^+$ ions in the APCI mass spectrum of (**a**) a mixture of *n*-propylamine and *n*-butylamine and (**b**) a mixture of cycloheptylamine and cyclooctylamine. Experiments performed using the LCQ ion trap [open circle = (M+1)$^+$; filled diamond = (2M+1–19)$^+$; asterisk = (2M+1)$^+$]. Circle in box = full scan mass spectrum [22].

From the experimental results, it appears that the (2M+1–19)$^+$ ions are formed in the course of ion/molecule reactions between protonated amines and neutral amines with associated losses of ammonia and molecular hydrogen. The resulting ions are likely to be protonated amines and imines, as already shown in eqs 1 and 2.

Product Characterization by Tandem Mass Spectrometry

CID was performed on the (2M+1–19)$^+$ ions generated by APCI in the LCQ ion trap in an attempt to confirm the hypothesis that protonated imines are generated. These ions were found to lose one or more neutral alkenes, which can be explained as the result of the loss of the alkyl group with hydrogen migration (eqs 3 and 4).

Table 1. Relative abundances of $(2M+1)^+$ ions and $(2M+1–19)^+$ ions[a] in APCI mass spectra using $CH_3OH/H_2O/HAc$ as mobile phase

Sample	$(2M+1–19)^+$ ions Th (relative abundance)	$(2M+1)^+$ ions Th (relative abundance)
n-Propylamine	100 (100)	119 (5)
n-Butylamine[b]	128 (30)	147 (2)
n-Hexylamine	184 (100)	203 (2)
n-Butylamine and *n*-propylamine[b]	100 (10)	119 (<0.5)
	114 (25)	133 (2)
	128 (50)	147 (2)
n-Butylamine and hexylamine	128 (10)	147 (<0.5)
	156 (85)	175 (2)
	184 (100)	223 (4)
n-Butylamine and *n*-amylamine[c]	128 (25)	147 (2)
	142 (88)	161 (<0.5)
	156 (85)	175 (<.0.5)
Cycloheptylamine	208 (100)	227 (0.5)
Cycloheptylamine and cylcooctylamine	208 (40)	227 (<0.5)
	222 (100)	241 (1.2)
	236 (60)	255 (<1)

[a]M is used to represent the neutral amine, and $(2M+1)^+$ indicates the proton-bound dimer.
[b]The base peak in both cases is protonated *n*-butylamine, 74 Th.
[c]The base peak is protonated *n*-amylamine, 88 Th.

$$R_1–CH_2CH_2CH_2–NH^+=CH–R_2 \rightarrow R_1–CH_2CH=CH_2 + H_2N^+=CH–R_2 \quad (3)$$

$$R_1–CH_2CH_2CH_2–NH^+=CH–R_2 \rightarrow R_1–CH=CH_2 + CH_3–N^+H=CH–R_2 \quad (4)$$

The CID results for a number of $(2M+1–19)^+$ ions are summarized in Table 2 and all are dominated by these relatively simple processes. As shown by the fragment ion abundances, the loss of the smaller alkene is almost always favored, presumably because of the greater stability of the resulting larger product ion. However, the loss of ethylene (C_2H_4) was not observed for the 100 Th ion (i.e., $C_2H_5–CH=NH^+–C_3H_7$): in other words, reaction 4 occurs only to a negligible extent when a propyl group is attached to the nitrogen atom. Literature data on the metastable decay and CID of iminium ions [23–25], generated by α-cleavage of alkylamine molecular ions, show alkene elimination as a major process and are consistent with the ion trap data that

Table 2. MS/MS data for $(2M+1–19)^+$ ions[a]

Sample	$(2M+1–19)^+$ ions Th (relative abundance)	CID fragments Th (relative abundance)	Resonance excitation voltage[c] (mV)
n-Propylamine	100 (100)	58 (50)	550 [11]
n-Butylamine	128 (100)	86 (32); 72 (13)	600 [12]
Hexylamine	184 (75)[b]	114 (100); 100 (70)	800 [16]
n-Butylamine and *n*-propylamine	100 (100)	58 (45)	550 [11]
	114 (20)	72 (100); 58 (22)	600 [12]
	128 (100)	86 (40); 72 (30)	600 [12]
n-Butylamine and hexylamine	128 (100)	86 (43); 72 (36)	600 [12]
	156 (100)[b]	114 (28); 100 (20); 86 (10)	700 [14]
	184 (80)[b]	114 (100); 100 (73)	800 [16]
n-Butylamine and *n*-amylamine	128 (100)	86 (43); 72 (35)	600 [12]
	142 (68)	100 (97); 86 (100); 72 (25)	650 [13]
	156 (100)	100 (56); 86 (33)	650 [13]
Cycloheptylamine	208 (70)	112 (100)	650 [13]
Cycloheptylamine and cyclooctylamine	208 (60)	112 (100)	650 [13]
	222 (100)	126 (60); 112 (48)	650 [13]
	236 (100)	126 (100)	650 [13]

[a]Data obtained using CID after APCI in an LCQ ion trap. Ions were isolated using a 2 Da/charge window unless specified otherwise.
[b]Data were obtained using a 4 Th isolation window.
[c]Data in brackets indicate the relative collision energy as read by the LCQ system.

correspond to dissociation under gentle activation conditions [26–28].

Confirmation of the hypothesis regarding the structures of the $(2M+1–19)^+$ ions required synthesis of authentic imines and study of their fragmentation after protonation. The authentic imines were synthesized and examined by APCI under the same conditions as used for the amine-derived $(2M+1–19)^+$ ions. Protonated imines were observed in the mass spectra, as expected, subsequently isolated and dissociated collisionally under similar conditions to those used for the corresponding $(2M+1–19)^+$ ions. A comparison of the CID spectra of the $(2M+1–19)^+$ ion, 114 Th, formed by APCI from the mixture of *n*-propylamine and *n*-butylamine and that of the corresponding protonated imines, is made in Figure 2. Figure 2a shows the product ion MS/MS spectrum of the 114 Th ion generated from the amine mixture, whereas Figure 2b, c show the MS/MS spectra of 114 Th ions produced by protonation of the authentic imines, **1** and **2:**

1 **2**

As mentioned earlier, whereas $[\mathbf{1}+H]^+$ should give 72 and 58 Th fragments, $[\mathbf{2}+H]^+$ should yield only the 72 Th fragment. The CID spectrum of the 114 Th ion produced from the amine mixture is consistent with contributions from both $[\mathbf{1}+H]^+$ and $[\mathbf{2}+H]^+$, as evidenced by the elevated 72 vs. 58 Th abundance ratio seen in Figure 2a compared to that in Figure 2b.

A similar comparison was also made for the cyclic amines. The CID product ion spectrum of the 222 Th ion, generated from a mixture of cycloheptylamine and cyclooctylamine, and the spectra of its counterpart protonated imines, are compared in Figure 3. The ion of 222 Th generated from the amine mixture gives fragments at 112 and 126 Th corresponding to the losses of cyclooctene and cycloheptene. On the other hand, the 222 Th ion resulting from protonation of the imine prepared from cyclooctylamine and cycloheptanone (Figure 3b) produces only the 112 Th ion under the same CID conditions. This fragment corresponds to C–N bond cleavage with the loss of cyclooctene according to reaction 3 proposed above. The C–C bond cleavage process, reaction 4, is not an expected pathway for the cycloalkyl group. An isomeric ion of 222 Th was produced by protonation of the imine synthesized from cycloheptylamine and cycloctanone. As expected, this ion fragments exclusively by the C–N cleavage route and, as shown in Figure 3c, produces only the 126 Th ion. These data confirm that the 222 Th signal produced from the mixture of cycloheptylamine and cycloctylamine is a mixture of two protonated isomeric imine ions and that isomerization does not occur during CID. Other $(2M+1–19)^+$ ions also showed analogous fragmentation behavior (Table 2) to the protonated imines (Table 3) and the data confirm the identification of these ions as protonated imines.

Additional experimental evidence for protonated imine formation came from experiments with tert-butylamine. This compound did not produce the $(2M+1–19)^+$ ion, instead a highly abundant $(2M+1–17)^+$ ion, 130 Th, was observed. This is an expected result because the absence of hydrogen atoms on the α-carbon atom does not allow elimination of H_2 by the mechanism illustrated in reaction 2. A comparison between the *n*-butylamine and tert-butylamine APCI spectra is shown in Figure 4. Note the much more intense proton-bound dimer (147 Th) in the tert-butylamine spectrum which can be attributed, in part at least, to the steric effect imposed by the tert-butyl group in the reaction.

Secondary amines were also examined to see if they undergo deamination analogously to primary amines. If such a process takes place, it will result in the elimination of a primary amine and a hydrogen molecule. The secondary amines diethylamine, dipropylamine, and *N*-methylcyclohexylamine were investigated under APCI conditions using the LCQ ion trap. In each case, primary amine elimination, a process that is analogous to ammonia loss in the primary amines, occurs although to a much smaller extent. The process is typically accompanied by a signal corresponding to further fragmentation by H_2 elimination. The reduced tendency for deamination may be because of a steric effect caused by the secondary amines. The expected deamination product ions themselves show characteristic fragmentations similar to that found for the primary amines. For example, dipropylamine examined in the APCI mode, led to the formation of 142 Th, which is the product of the losses of *n*-propylamine and molecular hydrogen from the proton-bound dimer of dipropylamine. Fragmentation of this ion, 142 Th, gave characteristic alkene losses to produce 114 Th (36% relative abundance) and 100 Th (30% relative abundance) analogous to the behavior of primary amines. By contrast, the proton-bound dimers again fragmented by CID to give only the protonated monomers. The data from the secondary amines studied are summarized in Table 4. Note that many other ions are also formed in low abundance under the APCI conditions and few have been characterized.

Electrospray and Chemical Ionization

Some of the primary amines, *n*-propylamine, *n*-butylamine, *n*-hexylamine, cyclohexylamine, and 2-methylcyclohexylamine, were examined using electrospray ionization in the quadrupole ion trap for comparison with the APCI data. In each case an $(2M+1–19)^+$ ion was observed and its product ion spectrum showed the same fragmentation behavior as seen in the correspond-

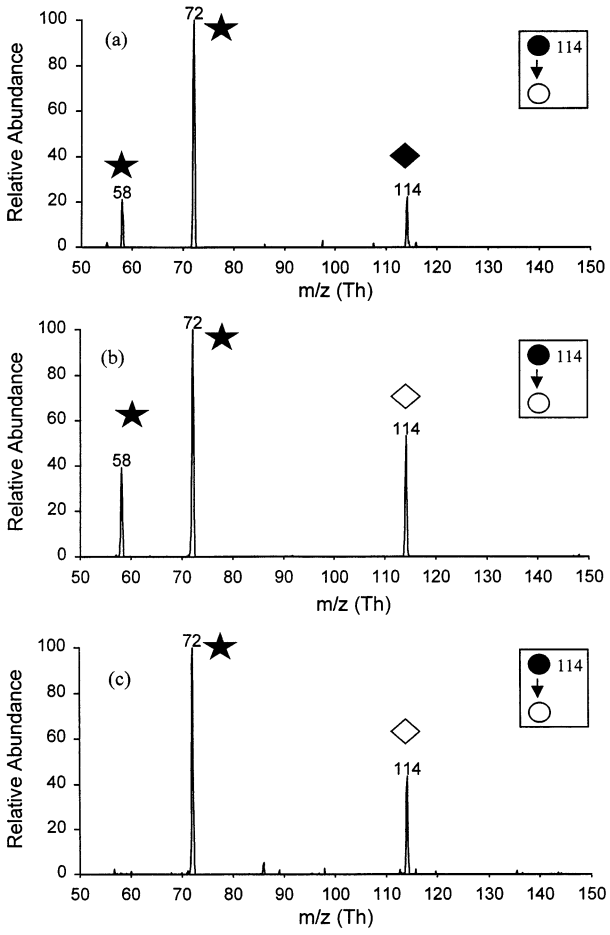

Figure 2. CID spectra recorded using APCI in the LCQ ion trap for (**a**) the $(2M+1–19)^+$ ion generated from a mixture of *n*-propylamine and *n*-butylamine], (**b**) the protonated imine $CH_3CH_2CH{=}NH^+CH_2CH_2CH_2CH_3$, and (**c**) the protonated imine $CH_3CH_2CH_2CH{=}NH^+CH_2CH_2CH_3$ [filled star = fragment ions; filled diamond = $(2M+1–19)^+$; open diamond = $(M+H)^+$ of imines]. Filled to open circle in box = product ion spectrum [22].

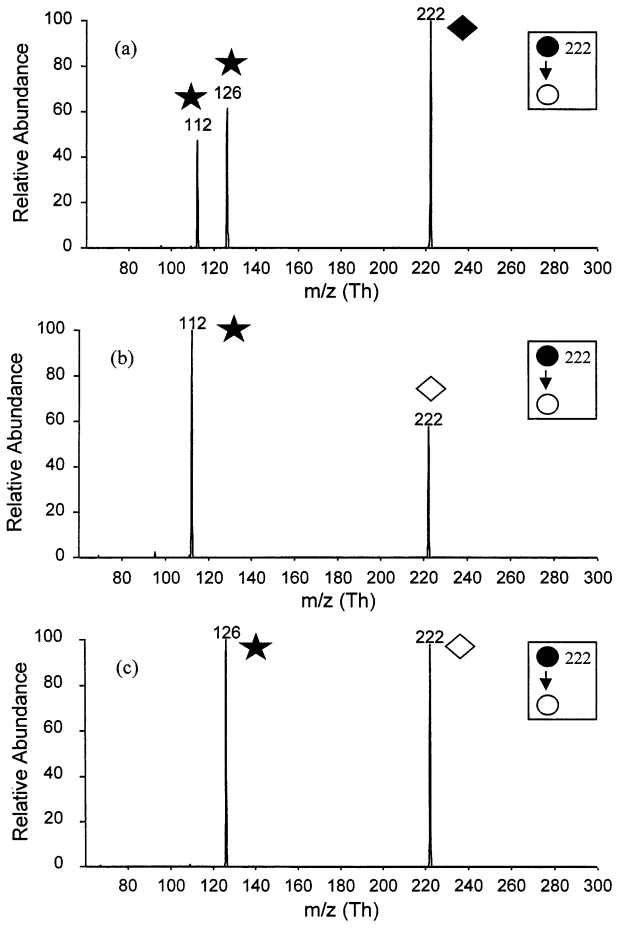

Figure 3. CID spectrum recorded using APCI in the LCQ ion trap for (**a**) the $(2M+1–19)^+$ ion generated from a mixture of cycloheptylamine and cyclooctylamine, (**b**) the protonated imine $C_8H_{15}NH^+{=}C_7H_{12}$, and (**c**) the protonated imine $C_7H_{13}NH^+{=}C_8H_{14}$ [filled star = fragment ions; filled diamond = $(2M+1–19)^+$; open diamond = $(M+H)^+$ of imines].

ing APCI experiment. It was also noticed that the formation of $(2M+1–19)^+$ ions in ESI occurred to an even greater extent than in APCI.

To determine whether the reaction leading to losses of NH_3 and H_2 can take place as purely gas-phase reactions, a triple quadrupole mass spectrometer, operating under CI conditions, was utilized to examine *n*-propylamine. Figure 5 compares the results of the APCI, ESI, and CI data of this compound, the CI data being taken using the triple quadrupole instrument using relatively high ion source sample pressures. It is evident that the APCI and ESI results are very similar. The CI data show a $(2M+1–19)^+$ ion although in relatively low abundance compared to $(2M+1)^+$ and even the proton-bound trimer $(3M+1–19)^+$ at 178 Th. Nevertheless, the presence of the deamination product and especially the large 159 Th peak, which corresponds to $(3M+1–19)^+$, clearly show that the reactions of interest do occur in the gas phase. Self-CI of a mixture of *n*-propylamine and *n*-butylamine, examined using the pentaquadrupole instrument, produced mainly proton-bound dimers with some $(2M+1–19)^+$ ions (~5%).

Isolation Efficiency and Type of Bonding

It was observed in all the CID experiments that the covalently bound ions, i.e., $(2M+1–19)^+$ ions, are far more stable than the proton-bound dimers. The two types of ions can be distinguished in the ion trap by their different isolation efficiencies (lower for the proton-bound dimers) and resonance excitation amplitudes needed for dissociation (lower for the proton-bound dimers). For the desirable 2 Th isolation window, the isolation efficiency is above 80% for covalently bound ions, but negligibly low for the proton-bound dimers. On the other hand, the resonance excitation voltage required to fragment a typical covalently bound ion in the LCQ ranged from 600 to 700 mV (12% to 14% relative collision energy), but for most proton-bound dimers, a value of only 300 mV (6% relative collision

Table 3. MS/MS data for protonated imines[a]

Imine	Protonated imine Th (relative abundance)	CID fragments Th (relative abundance)	Resonance excitation voltage[b] (mV)
$C_3H_7N{=}CHC_2H_5$	100 (100)	58 (82)	550 [11]
$C_4H_9N{=}CHC_2H_5$	114 (55)	72 (100); 58 (40)	600 [12]
$C_3H_7N{=}CHC_3H_7$	114 (45)	72 (100)	600 [12]
$C_7H_{13}N{=}C_6H_{11}$	194 (60)	98 (100)	600 [12]
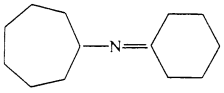			
$C_8H_{14}N{=}C_7H_{13}$	222 (60)	112 (100)	650 [13]
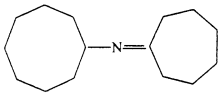			
$C_7H_{12}N{=}C_8H_{15}$	222 (96)	126 (100)	650 [13]
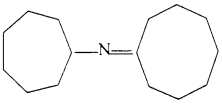			

[a]Data were obtained using CID after APCI in an LCQ ion trap.
[b]Data in brackets indicate the relative collision energy as read by the LCQ system.

energy) was adequate to cause some fragmentation and 450 mV (9% relative collision energy) was enough for complete fragmentation.

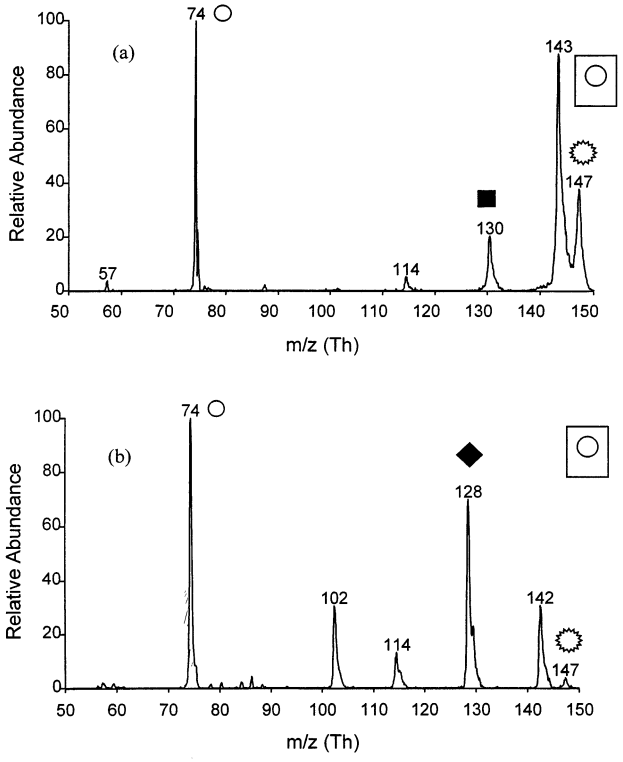

Figure 4. APCI mass spectra recorded using the LCQ ion trap (**a**) tert-butylamine and (**b**) *n*-butylamine [open circle = $(M+1)^+$; filled square = $(2M+1–17)^+$; filled diamond = $(2M+1–19)^+$; asterisk = $(2M+1)^+$].

Considering that space charge effects [29, 30] shift the resonant frequency of the ion and so might be responsible for the low isolation efficiency of the proton-bound dimers, a three stage stepwise isolation process was attempted to increase the isolation efficiency. This continued to give unsatisfactory results when the isolation window was narrowed in the last stage. For example, the isolation efficiency of the *n*-propylamine homodimer (119 Th) was only 15% even at a window size of 10 Th, whereas other dimers gave even poorer isolation efficiencies. These facts suggest that the proton-bound dimer ions are relatively unstable under the isolation conditions, because of their weak bonding. These properties can be utilized in the LCQ experiments to distinguish the types of ions present in the mass spectrum.

Effects of the Mobile Phase

With pure methanol as the mobile phase, $(2M+1–19)^+$ ions were generated in the highest abundance compared to data obtained when methanol/water and methanol/water/acetic acid were used. The acidic $CH_3OH/H_2O/HOAc$ mobile phase slightly increased proton-bound dimer formation but the formation of $(2M+1–19)^+$ ions was greatly suppressed. When ammonium acetate was used, the formation of $(2M+1–19)^+$ ions was completely suppressed. These effects are illustrated in Figure 6a–c in the case of *n*-butylamine APCI. In addition, when ammonium acetate was used instead of acetic acid in the mobile phase, the proton-bound dimers were formed with greater abundance, and better isolation was achieved, although still only

Table 4. Mass spectra of some secondary amines[a,b]

Compounds	Expected product ions (Th) after (RNH_2+H_2) losses	Product ions (Th and relative abundance)
Diethylamine	100	74 (100); 86 (38); 100 (3.0); 102 (9.4); 111 (3.4); 126 (2.0); 129 (10); 130 (4.3); 138 (10.5); 143 (2.0); 147 (1.8); 150 (4.6)
Dipropylamine	142	102 (100); 103 (8); 114 (50); 115 (5); 142 (5); 150 (5); 171 (2); 195 (2); 203 (3); 213 (4.3)
N-Methyl cyclohexylamine	126, 194	83 (3); 110 (10.5); 112 (62.4); 114 (100); 115 (7.5); 126 (28); 128 (2.7); 141 (1); 155 (6.6); 180 (3); 196 (1.2); 207 (3); 219 (3); 223 (26); 224 (10); 227 (3.6); 237 (12.5); 237 (12.5); 238 (5.7)

[a]Data were obtained using ESI in an LCQ ion trap.
[b]The underlined ions indicate the expected (RNH_2+H_2) loss product ions.

when large isolation windows (10 Th) were used. For example, the use of ammonium acetate increased the formation of *n*-butylamine proton-bound dimer by 40% compared to when acetic acid was used, and deamination was completely suppressed. The ammonium acetate and acetic acid data suggest that the formation of the $(2M+1–19)^+$ ions is competitive with proton-bound dimer formation.

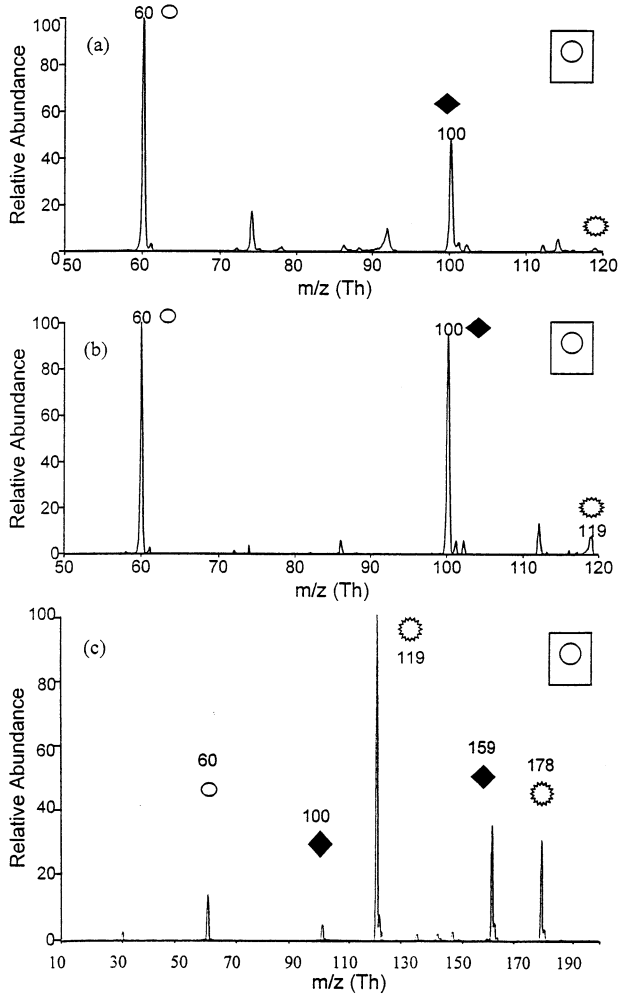

Figure 5. Mass spectra of *n*-propylamine using different ionization techniques: (**a**) APCI in the LCQ ion trap, (**b**) ESI in the LCQ ion trap, and (**c**) self-CI in the triple quadrupole [open circle = $(M+1)^+$; filled diamond = $(2M+1–19)^+$ or $(3M+1–19)^+$; asterisk = $(2M+1)^+$ or $(3M+1)^+$].

Mechanisms

Because APCI and ESI involve both solution and gas-phase processes [31, 32], these are not the best ionization methods to use to clarify the origin of the $(2M+1–19)^+$ ions. In addition, it is possible that $M^{+\cdot}$, $(M+1)^+$, and $(M-1)^+$ are all formed in the initial stages of the ionization, and one or more of these ions may lead to the $(2M+1–19)^+$ ion formation. Attempts to isolate the protonated amine under APCI conditions and examine its reactions with neutral amines in the LCQ failed, probably because of the very low amine pressure in the ion trap ($P \sim 1.5 \times 10^{-5}$ torr, mostly water).

For these reasons, an ion trap instrument equipped with internal ionization, the ITS 40 was used for most of the mechanistic studies. At relatively high amine pressures (a few mtorr), using a scan function but corresponding nominally to electron ionization, the protonated amine was generated in relatively high abundance through self-CI. The $(2M+1–19)^+$ ion was also produced if a delay period was allowed for ion/molecule reactions before mass analysis. Figure 7a shows the mass spectrum of *n*-butylamine (with *n*-amylamine residue in the ion trap) under self-CI conditions (60 ms delay for ion/molecule reactions). The base peak at m/z 74 corresponds to protonated *n*-butylamine, and the peak at m/z 88 is because of protonated *n*-amylamine. Three $(2M+1–19)^+$ ions occur corresponding to the deamination plus dehydrogenation products of the dimer of *n*-butylamine, the heterodimer of *n*-butylamine and *n*-amylamine, and the dimer of *n*-amylamine. The only proton-bound dimer observed was that of *n*-butylamine. The ion/molecule reactions of several protonated amines have also been examined using the ITS 40. These ions were isolated and allowed time to react, and this led to the formation of both $(2M+1–19)^+$ ions and the proton-bound dimer. Figure

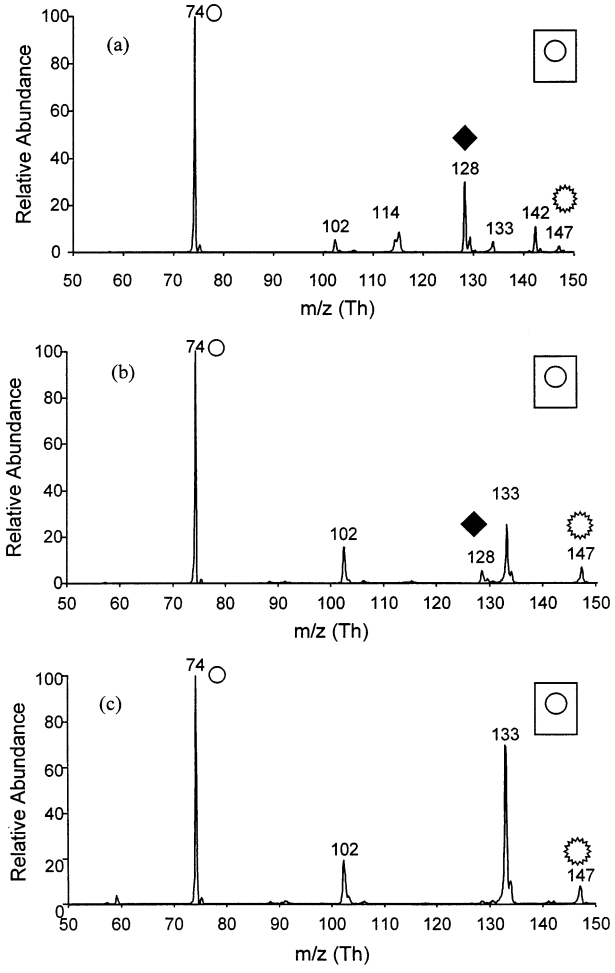

Figure 6. Mass spectra of *n*-butylamine recorded using the LCQ ion trap and different APCI conditions: (**a**) 1% acetic acid in 50:50 methanol/water, (**b**) 1% ammonium acetate in 50:50 methanol/water, and (**c**) a higher concentration of ammonium acetate [full circle = $(M+1)^+$; filled diamond = $(2M+1–19)^+$; asterisk = $(2M+1)^+$].

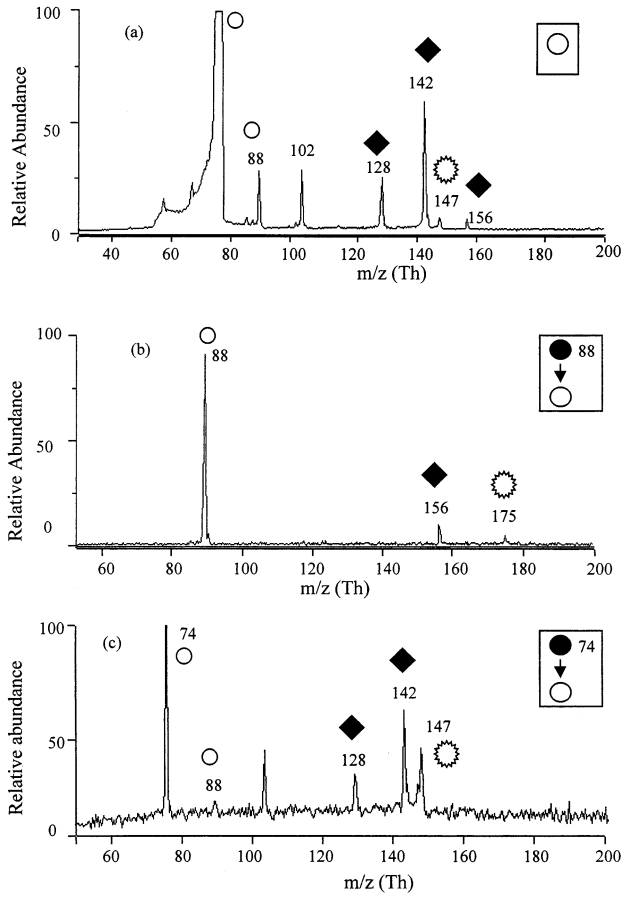

Figure 7. (**a**) Mass spectrum of *n*-butylamine (with residual *n*-amylamine) recorded using the ITS ion trap: ionization time, 1 ms; reaction time, 60 ms. (**b**) Ion/molecule reaction product ion spectrum of protonated *n*-amylamine recorded after reaction with the neutral compound for 180 ms in the ITS ion trap. (**c**) Ion/molecule reaction product ion spectrum of isolated protonated *n*-butylamine recorded after reaction with neutral *n*-butylamine (and residual *n*-amylamine) for 180 ms in the ITS ion trap [open circle = $(M+1)^+$; filled diamond = $(2M+1–19)^+$; asterisk = $(2M+1)^+$].

7b shows the ion/molecule product spectrum for reaction of protonated *n*-amylamine (88 Th) with the corresponding neutral amine. When a 180 ms reaction period was used, both $(2M+1–19)^+$ (156 Th) and the proton-bound dimer (175 Th) were formed. Extended reaction times increased the signals for both ions, again indicating that they are competitive reactions. An example is shown in Figure 7c for protonated *n*-butylamine. Note that 88 Th is because of the protonation of residual *n*-amylamine in the ion trap. After prolonged reaction times, more $(2M+1–19)^+$ ion was observed along with proton-bound dimer. These results clearly show that the $(2M+1–19)^+$ ions are formed from the protonated amine through gas phase ion/molecule reactions.

Clean isolation of the amine cation $M^{+\cdot}$ failed in the ITS 40, simply because of the high reactivity of the radical cations and the relatively high amine neutral pressure in the ion trap. Even the best isolation achived still showed two ions—the radical cation and the protonated amine—suggesting that the protonated amine is produced from the radical cation. Other experiments have shown that, allowing more time for reaction, the radical cation reacts completely to the protonated amine. Ion/molecule reactions were also attempted in the pentaquadrupole instrument equipped with an EI source. The radical cation of *n*-butylamine (73 Th) was isolated in one quadrupole and reacted with *n*-hexylamine in another quadrupole. The deamination product ion at m/z 156, the corresponding $(2M+1–19)^+$ ion, was not observed and we conclude that the radical cation can be ruled out as a precursor of the $(2M+1–19)^+$ ions. To see if the $(M-1)^+$ ions might serve as a precursor ion for the $(2M+1–19)^+$ ions, the corresponding $(M-1)^+$ ion of ethylamine (44 Th) was generated from *s*-butylamine in the ITS 40 ion trap and isolated using apex isolation.

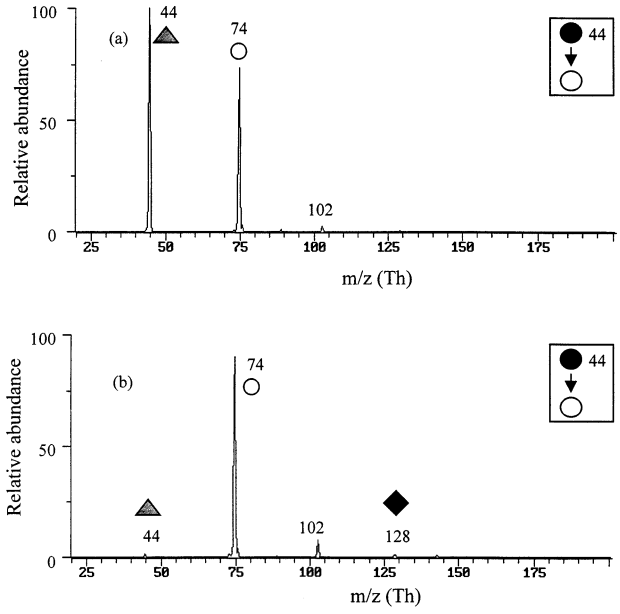

Figure 8. (**a**) Ion/molecule reaction product ion spectrum (20 ms) of m/z 44 ion generated by fragmentation of *s*-butylamine with neutral compounds *s*-butylamine, *n*-amylamine, and dipropylamine and recorded using the ITS ion trap. (**b**) 120 ms reaction time showing that the formation of protonated amine which appears first before any $(2M+1–19)^+$ is observed [open circle = $(M+1)^+$; filled diamond = $(2M+1–19)^+$; filled triangle = $(M - 1)^+$].

Reaction of these ions with neutral amines did not lead to the formation of $(2M+1–19)^+$ ions but rather resulted in the formation of protonated amines, as shown in Figure 8a. At longer reaction times, the deamination product ion occurs as illustrated in Figure 8b, but it appears that the $(2M+1–19)^+$ ion is formed from the protonated amine rather than directly from $(M - 1)^+$. Otherwise, one would expect to observe m/z 100 because of the loss of ammonia from the adduct of ion 44 Th and *n*-butylamine (MW 73). From these results one must conclude that it is indeed $(M+H)^+$ and not $M^{+\cdot}$ or $(M - H)^+$ that is the reagent ion involved in the deamination reaction.

The CID spectra of the proton-bound dimers show only the protonated amines as fragmentation products; data are shown in Table 5. Homodimers of the amines fragment to give the protonated monomers exclusively in cases of *n*-butylamine and cycloheptylamine. For the heterodimers, two fragment ions appear if their proton affinities are sufficiently similar, such as in the case of *n*-amylamine and *n*-heptylamine. The amines with higher proton affinity have higher abundances, as a result of competitive fragmentations controlled largely by product ion stability [11, 12]. On the other hand, if the proton affinities of the amines differ substantially, only the amine with higher proton affinity is observable in the CID spectra. The absence of deamination products from dissociation of the proton-bound dimer is in contrast to the behavior of the corresponding alcohols, which show dehydration products [33]. Only the protonated amine can lead directly to the formation of the deamination products and it appears that this is a kinetically controlled process with which may have an activation energy barrier. Because the secondary amines displayed less deamination, it is inferred that the reaction has strict steric requirements. This is consistent with the proposal that it occurs by nucleophilic substitution at the α-carbon.

The reaction enthalpies for the simple deamination reaction and the deamination and dehydrogenation reaction leading to the protonated imine were estimated for the case of *n*-propylamine (i.e., eqs 1 and 2, R_1=R_2=C_2H_5). The thermochemical data used in these estimates is summarized in Table 6; note the use of group equivalent methods to estimate the proton affinity of the imine. The reaction enthalpies are estimated to be −67 and −73 kJ/mol, respectively. No attempts have been made to calculate the potential energy surfaces although it is noted that Audier [34] has reported a 52 kJ/mol barrier for what may be a similar reaction, eq 5.

$$CH_2–CH_2–NH_3^+ + CH_3–CH_2–NH_2 \rightarrow \cdot CH_2–CH_2–NH_2^+–CH_2–CH_3 + NH_3 \quad (5)$$

Table 5. MS/MS data for the proton-bound dimers[a]

Amine 1	Amine 2	PBD[b] (Th)	Proton affinity difference (kJ/mol)[c]	Fragment ions (Th and relative abundance)
n-Butylamine		147		74 (exclusively)
Cycloheptylamine		227		114 (exclusively)
n-Amylamine	*n*-heptylamine	203	0.1	88 (24.5); 116 (53)
n-Butylamine	*n*-amylamine	161	0.7	74 (15); 88 (100)
n-Propylamine	*n*-butylamine	133	3.6	74 (exclusively)
n-Propylamine	*n*-heptylamine	175	4.4	114 (exclusively)

[a]Proton-bound dimers were generated in ESI in LCQ, mass selected and dissociated by CID.
[b]PBD = proton-bound dimers.
[c]Proton affinity values [35] of *n* = propylamine, *n*-butylamine, *n*-amylamine, and *n*-heptylamine are 917.8, 921.4, 922.1, and 922.2 kJ/mol, respectively.

Table 6. Thermochemical data used to estimate the reaction enthalpies[a]

Compounds	Proton affinity (kJ/mol)	$\Delta H_f^\circ g$ (kJ/mol)
$CH_2{=}NH$	852.9	
$CH_3CH{=}NH$	885.1	
$(CH_3)_2C{=}NH$	932.3	
$CH_3CH{=}NCH_2CH_3$	941.9	
$(CH_3)_2C{=}NCH_2CH_3$	976.0	
$CH_3CH_2CH_2CH{=}NCH_2CH_3$	955.5	
$CH_3CH_2CH_2NH_2$	917.8	−69.9
$(CH_3CH_2CH_2)_2NH$	962.3	−116.1[b]
NH_3		−45.94
H^+		1536.248
$CH_3CH_2CH_2N{=}CHCH_2CH_3$	970[d]	−196.9[c]

[a]The thermochemical data are taken from the NIST WebBook [36].
[b]The value was calculated from the $\Delta H_f^\circ(l)$ value of dipropylamine and its vaporization enthalpy that are −156.2 and 40.1 kJ/mol.
[c]The data were calculated from the following reaction with $\Delta H_{rxn} = 80.8$ kJ/mol: $CH_3CH_2CH_2N{=}CHCH_2CH_3 + H_2 \rightarrow (CH_3CH_2CH_2)_2NH$.
[d]The proton affinity was estimated using group equivalent methods from the known imine proton affinities.

The shape of this potential energy surface is not known.

An unresolved, and perhaps related issue, is the connection between the processes leading to the $(2M+1–17)^+$ and $(2M+1–19)^+$ ions. Indirect evidence that the loss of molecular hydrogen follows the loss of ammonia is provided by the tert-butylamine case, in which only $(2M+1–17)^+$ is observed in the mass spectrum (Figure 4a). However, CID of protonated dipropylamine in the LCQ ion trap did not lead to the elimination of H_2. To address this point further, the ion/molecule reactions of the *n*-butyl cation with *n*-butylamine (and *n*-amylamine) were examined (Figure 9). In this case the intact adduct corresponds to the $(2M+1–17)^+$ ion of the earlier spectra and not only is it observed but it is accompanied by an ion due to H_2 elimination, viz. the analog of $(2M+1–19)^+$. Similar results were obtained when the cyclohexane cation was reacted with cyclohexylamine. These results are interesting because they provide independent evidence that H_2 elimination is associated with deamination.

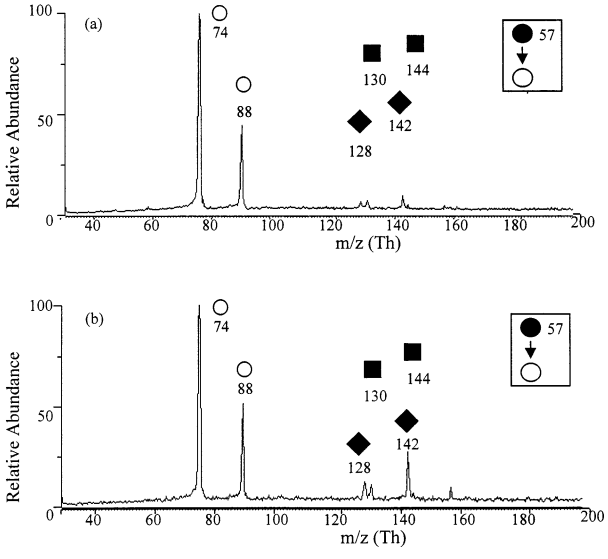

Figure 9. Ion/molecule reaction product ion spectrum of mass-selected $C_4H_9^+$ generated from *n*-chlorobutane with *n*-butylamine and *n*-amylamine (ITS ion trap) (**a**) reaction time 60 ms and (**b**) reaction time 120 ms [open circle = $(M+1)^+$; filled diamond = $(2M+1–19)^+$; filled square $(2M+1–17)^+$].

Conclusion

(1) Gas phase ion/molecule reactions of amines under APCI, ESI, and CI conditions lead to deamination and protonated imine formation. Because of the complicated nature of APCI and ESI, it is not possible to exclude the occurrence of this reaction in the solution phase, however, ion/molecule reactions in the gas phase demonstrate that the protonated amine is the direct precursor ion for both product ions.

(2) Deamination apparently occurs by a nucleophilic substitution mechanism although the reaction energetics are not fully characterized.

(3) Deamination is often followed by dehydrogenation to give the characteristic $(2M+1–19)^+$ ions unless structural features are chosen to preclude it (as in tert-butylamine). The reaction of the *n*-butyl cation with *n*-butylamine demonstrates that dehydrogenation can follow formation of the deamination product. Nevertheless, direct conversion of the proposed primary deamination products, $(2M+1–17)^+$, to the corresponding protonated imines could not be demonstrated by CID.

(4) Proton-bound dimer formation is competitive with deamination and excitation of the dimer does not lead to the protonated imine.

(5) The protonated imines undergo characteristic C–N and C–C cleavages with associated alkene losses in the ion trap under CID conditions.

(6) Although isolation of the protonated imines is readily performed, the isolation efficiency of the proton-bound dimers is low because of their weak binding. These bonds do not readily withstand the isolation conditions present in the ion trap mass spectrometer.

(7) Isolation efficiency and the amplitude of the voltage needed for CID resonant excitation serve as diagnostics to distinguish loosely-bonded ions, represented by proton-bound dimers, from covalently bound ions, represented by the protonated imines.

Acknowledgments

This work was supported by the Office of Naval Research and by the National Science Foundation, CHE-9732670. We thank Feng Wang, J. M. Wells, and P. D. Thomas for helpful discussions. The referees are thanked for particularly insightful comments.

References

1. Munson, M. S. B.; Field, F. H. *J. Am. Chem. Soc.* **1966,** *88*, 2621–2630.
2. Harrison, A. G. *Chemical Ionization Mass Spectrometry*; CRC: Boca Raton, FL, 1992.
3. Field, F. H. *J. Am. Chem. Soc.* **1970,** *92*, 2672–2676.
4. Herman, J. A.; Harrison, A. G. *Can. J. Chem.* **1981,** *59*, 2125–2131.
5. Jardine, I.; Catherine, F. *J. Am. Chem. Soc.* **1976,** *98*, 5086–5089.
6. Reiner, E. J.; Poirier, R. A.; Peterson, M. R.; Csizmadia, I. G.; Harrison, A. G. *Can. J. Chem.* **1986,** *64.*, 1652–1660.
7. Sigsby, M. L.; Day, R. J.; Cooks, R. G. *Org. Mass Spectrom.* **1979,** *14*, 556–561.
8. Tedder, J. M.; Walker, G. S. *J. Chem. Soc. Perkin Trans. 2* **1991**, 317–320.
9. Kaltashov, I. A.; Fenselau, C. C. *Int. J. Mass Spectrom. Ion Processes* **1995,** *146/147*, 339–347.
10. Li, X.; Harrison, A. G. *Org. Mass Spectrom.* **1993,** *28*, 366–371.
11. Cooks, R. G.; Kruger, T. L. *J. Am. Chem. Soc.* **1977,** *99*, 1279–1281.
12. Cooks, R. G.; Patrick, J. S.; Kotiaho, T.; McLuckey, S. A. *Mass Spectrom. Rev.* **1994,** *13*, 287–339.
13. Audier, H. E.; Millet, A.; Perret, C.; Tabet, J.-C.; Varenne, P. *Org. Mass Spectrom.* **1978,** *13*, 315–318.
14. Davis, D. V.; Cooks, R. G. *Org. Mass Spectrom.* **1981,** *16*, 176–179.
15. Wysocki, V. H.; Burinsky, D. J.; Cooks, R. G. *J. Org. Chem.* **1985,** *50*, 1287–1291.
16. Milne, G. W. A.; Axenrod, T.; Fales, H. M. *J. Am. Chem. Soc.* **1970,** *92*, 5170–5175.
17. Cleven, C. D.; Hoke, S. H.; Cooks, R. G.; Hrovat, D. A.; Smith, J. M.; Lee, M. S.; Borden, W. T. *J. Am. Chem. Soc.* **1996,** *118*, 10872–10878.
18. Brodbelt-Lustig, J. S.; Cooks, R. G. *Talanta* **1989,** *36*, 255–260.
19. Nourse, B. D.; Cooks, R. G. *Int. J. Mass Spectrom. Ion Processes* **1991,** *106*, 249–272.
20. Schwartz, J. C.; Schey, K. L.; Cooks, R. G. *Int. J. Mass Spectrom. Ion Processes* **1990,** *101*, 1–20.
21. Cooks, R. G.; Rockwood, A. L. *Rapid Commun. Mass Spectrom.* **1991,** *5*, 93.
22. Schwartz, J. C.; Wade, A. P.; Enke, C. G.; Cooks, R. G. *Anal. Chem.* **1990,** *62*, 1809–1818.
23. Hammerum, S.; Kuck, D.; Derrick, P. J. *Tetrahedron Lett.* **1984,** *25*, 893–896.
24. Bowen, R. D. *Mass Spectrom. Rev.* **1991,** *10*, 225–279.
25. Gross, J. H.; Veith, H. H. *Org. Mass Spectrom.* **1993,** *28*, 867–872.
26. Louris, J. N.; Cooks, R. G.; Syka, J. E. P.; Kelly, P. E.; Stafford, G. C.; Todd, J. F. J. *Anal. Chem.* **1987,** *59*, 1677–1685.
27. March, R. E.; Todd, J. F. J. *Practical Aspects of Ion Trap Mass Spectrometry, Vol. I: Fundamentals of Ion Trap Mass Spectrometry*; CRC: Boca Raton, FL, 1995.
28. Vekey, K. *J. Mass Spectrom.* **1996,** *31*, 445–463.
29. Cox, K. A.; Cleven, C. D.; Cooks, R. G. *Int. J. Mass Spectrom. Ion Processes* **1995,** *144*, 47–65.
30. Mo, W.; Todd, J. F. J. *Rapid Commun. Mass Spectrom.* **1996,** *10*, 424–428.
31. Fenn, J. B.; Mann, M.; Meng, C. K.; Wong, S. F.; Whitehouse, C. M. *Mass Spectrom.* Rev. **1990,** *9*, 37–70.
32. Bruins, A. P. *Mass Spectrom. Rev.* **1991,** *10*, 53–77.
33. Iraqui, M.; Lifshitz, C. *Int. J. Mass Spectrom. Ion Processes* **1989,** *88*, 45–57.
34. Audier, H. E.; Fossey, J.; Leblanc, D.; Mourgues, P. *Bull. Soc. Chim. Fr.* **1996,** *133*, 59–64.
35. Hunter, E. P.; Lias, S. G. *J. Phys. Chem. Ref. Data* to be published.
36. Mallard, W. G.; Linstrom, P. J. *NIST Chemistry WebBook, NIST Standard Reference Database, Number 69*; National Institute of Standards and Technology: Gaithersburg, MD 20899 (http://webbook.nist.gov), 1998.